

# Longitudinal magnon in the tetrahedral spin system $\text{Cu}_2\text{Te}_2\text{O}_5\text{Br}_2$ near quantum criticality

C. Gros,<sup>1</sup> P. Lemmens,<sup>2,4</sup> M. Vojta,<sup>3</sup> R. Valentí,<sup>1</sup> K.-Y. Choi,<sup>4</sup> H. Kageyama,<sup>5</sup> Z. Hiroi,<sup>5</sup> N. V. Mushnikov,<sup>5</sup> T. Goto,<sup>5</sup> M. Johnsson,<sup>6</sup> and P. Millet<sup>7</sup>

<sup>1</sup>Fakultät 7, Theoretische Physik, Universität des Saarlands, D-66041 Saarbrücken, Germany

<sup>2</sup>Max Planck Institute for Solid State Research, D-70569 Stuttgart, Germany

<sup>3</sup>Theoretische Physik III, Universität Augsburg, D-86135 Augsburg, Germany

<sup>4</sup>2. Physikalisches Institut, RWTH Aachen, D-52056 Aachen, Germany

<sup>5</sup>Institute for Solid State Physics, Univ. of Tokyo, Kashiwa-shi, Chiba 277-8581, Kashiwa, Japan

<sup>6</sup>Department of Inorganic Chemistry, Stockholm Univ., S-10691 Stockholm, Sweden

<sup>7</sup>Centre d'Elaboration de Matériaux et d'Etudes Structurales, CEMES/CNRS, F-31062 Toulouse, France

(Received 28 January 2003; published 8 May 2003)

We present a comprehensive study of the coupled tetrahedra compound  $\text{Cu}_2\text{Te}_2\text{O}_5\text{Br}_2$  by theory and experiments in external magnetic fields. We report the observation of a longitudinal magnon in Raman scattering in the ordered state close to quantum criticality. We show that the excited tetrahedral-singlet sets the energy scale for the magnetic ordering temperature  $T_N$ . This energy is determined experimentally. The ordering temperature  $T_N$  has an inverse-log dependence on the coupling parameters near quantum criticality.

DOI: 10.1103/PhysRevB.67.174405

PACS number(s): 75.30.Gw, 75.10.Jm, 78.30.-j

## INTRODUCTION

Quantum fluctuations in antiferromagnetic insulators lead to a reduction of the magnetic moment and to a new mode in which the magnitude of the local order parameter oscillates: the longitudinal magnon (LM) (Ref. 1) [see Fig. 1(a)]. This elementary excitation is absent in classical magnets, where the excitations perform a precession of the moment around its equilibrium position and are therefore transversally polarized [see Fig. 1(b)]. The longitudinal mode is difficult to observe and only recently has a LM been detected by inelastic neutron scattering in quantum spin- $\frac{1}{2}$  (Refs. 2 and 3) and spin-1 (Refs. 4 and 5) chain compounds.

Quantum spin fluctuations are of special importance in quasi-zero-dimensional systems with weakly coupled spin clusters. These lattices allow for quantum phase transitions between magnetically ordered states and nonmagnetic phases with a spin gap.<sup>6</sup> The recently discovered<sup>7</sup> spin-tetrahedral compounds  $\text{Cu}_2\text{Te}_2\text{O}_5\text{X}_2$  ( $X=\text{Cl}, \text{Br}$ ) have been shown to order at transition temperatures  $T_N^{(\text{Cl})}=18.2$  K and  $T_N^{(\text{Br})}=11.4$  K which are strongly suppressed with respect to the magnitude of the intratetrahedral couplings.<sup>8</sup> Unconventional Raman scattering has been found in the magnetic channel,<sup>8,9</sup> and the occurrence of low-lying singlet excitations has been proposed.<sup>7</sup> Plateaus in the magnetization have been predicted for a related linear chain of spin tetrahedra.<sup>10</sup>

The nature of the ordered states in  $\text{Cu}_2\text{Te}_2\text{O}_5\text{X}_2$  has not yet been settled. The ordering temperatures  $T_N^{(\text{Cl})}$  and  $T_N^{(\text{Br})}$  decrease and rise, respectively, with an external magnetic field.<sup>8</sup> This unusual magnetic-field-induced stabilization of  $T_N^{(\text{Br})}$  motivated in part the present study. A decrease of  $T_N$  is typical for an antiferromagnet in the classical limit. We will show later on that  $T_N$  may rise near a quantum phase transition. This results then indicates  $\text{Cu}_2\text{Te}_2\text{O}_5\text{Br}_2$  to be close to criticality.

Here we report the observation of a LM in  $\text{Cu}_2\text{Te}_2\text{O}_5\text{Br}_2$  by Raman scattering in a magnetic field, and present the

evolution of this mode under the influence of an external magnetic field. We believe that this study constitutes the first time that a longitudinal magnon is detected optically, as well as the first observation of such a mode in a tetrahedral spin system, i.e., in a system with an even number of spins per unit cell. Furthermore, high-field magnetization and other thermodynamic data on pure and substituted  $\text{Cu}_2\text{Te}_2\text{O}_5(\text{Br}_x\text{Cl}_{1-x})_2$  are compared via a mean-field analysis which allows one to determine the microscopic parameters for  $\text{Cu}_2\text{Te}_2\text{O}_5\text{Br}_2$ . We find, interestingly, that the scale of the ordering temperature  $T_N$  is set by the (nonmagnetic) excited singlet of the copper tetrahedron and that  $T_N$  has an essential singularity at criticality.

## MEAN-FIELD APPROACH

We assume that the basic spin cluster in this compound is given by the copper tetrahedron (see the inset in Fig. 2). We denote by  $s_{kl}$  the spin-singlet state of two intratetrahedral sites  $k$  and  $l$ , and by  $t_{kl}^\alpha$  the respective triplet states, with  $\alpha=\pm 1, 0$ . We start by considering the eigenstates of the isolated tetrahedra with  $H_t=J_1[(\mathbf{S}_1+\mathbf{S}_2)\cdot(\mathbf{S}_3+\mathbf{S}_4)]+J_2(\mathbf{S}_1\cdot\mathbf{S}_2+\mathbf{S}_3\cdot\mathbf{S}_4)$ , which consist of two singlets, three triplets, and one quintuplet.

For  $J_2 < J_1$  the ground state singlet  $\psi_{s_1}$  and the excited singlet  $\psi_{s_2}$  are

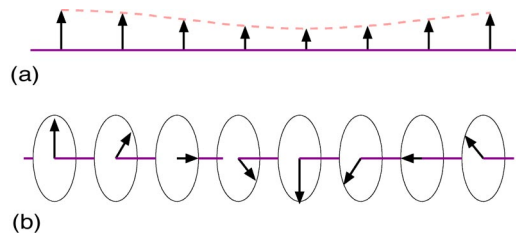


FIG. 1. Schematic representation of (a) a longitudinal magnon and (b) a transversal magnon.

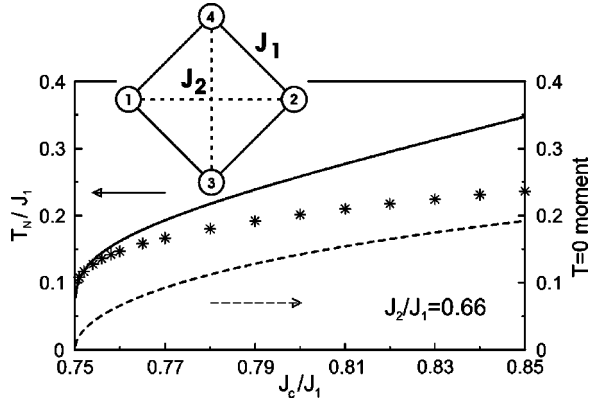


FIG. 2. Néel temperature (left scale) and spin tetrahedra mean-field moment (right scale) for  $J_2/J_1=0.66$ . Shown is the analytic approximation to leading order by Eq. (7) (solid line) and the numerical solution of the self-consistency equation (6) (stars). The dashed line (right scale) is the magnetic moment at zero-temperature equation (8). Note the logarithmic singularity in  $T_N$  for  $J_c \rightarrow 0.75J_1$ . Inset: Cu tetrahedron with exchange couplings  $J_1$  and  $J_2$  (solid and dashed lines).

$$\psi_{s_1} = \frac{-1}{\sqrt{3}} [t_{12}^0 t_{34}^0 - t_{12}^+ t_{34}^- - t_{12}^- t_{34}^+], \quad \psi_{s_2} = s_{12} s_{34} \quad (1)$$

with eigenenergies  $E_{s_1} = -2J_1 + J_2/2$  and  $E_{s_2} = -3J_2/2 = E_{s_1} + \Delta E_{s_2}$ , with  $\Delta E_{s_2} = 2J_1 - 2J_2$ . The three triplets  $\psi_{t_{11}}^\alpha$ ,  $\psi_{t_{12}}^\alpha$ , and  $\psi_{t_{13}}^\alpha$  have the (excitation) energies  $\Delta E_{t_1} = J_1$  and  $\Delta E_{t_2} = \Delta E_{t_3} = 2J_1 - J_2$ , with respective eigenstates

$$\begin{aligned} \psi_{t_{11}}^0 &= \frac{1}{\sqrt{2}} (t_{12}^+ t_{34}^- - t_{12}^- t_{34}^+), \\ \psi_{t_{11}}^- &= \frac{1}{\sqrt{2}} (t_{12}^0 t_{34}^- - t_{12}^- t_{34}^0), \\ \psi_{t_{11}}^+ &= \frac{1}{\sqrt{2}} (t_{12}^+ t_{34}^0 - t_{12}^0 t_{34}^+), \\ \psi_{t_{12}}^\alpha &= s_{12} t_{34}^\alpha, \quad \psi_{t_{13}}^\alpha = t_{12}^\alpha s_{34}. \end{aligned} \quad (2)$$

The quintuplet has the energy  $\Delta E_q = 3J_1$ . The intertetrahedra couplings can be described in a mean-field approach by<sup>12</sup>

$$H_{MF} = -J_c M (S_1^z + S_2^z - S_3^z - S_4^z)$$

and

$$M = \frac{1}{4} \langle S_1^z + S_2^z - S_3^z - S_4^z \rangle, \quad (3)$$

with  $M$  being the staggered magnetization order parameter.  $J_c$  here is the sum over all intertetrahedra couplings.

The mean-field Hamiltonian  $H_{MF}$  couples  $\psi_{s_1}$  and  $\psi_{t_{11}}^0$ , leading to new eigenstates for  $H = H_t + H_{MF}$ ,

$$|\varphi\rangle = \cos \varphi |\psi_{s_1}\rangle + \sin \varphi |\psi_{t_{11}}^0\rangle,$$

$$|\bar{\varphi}\rangle = \sin \varphi |\psi_{s_1}\rangle - \cos \varphi |\psi_{t_{11}}^0\rangle, \quad (4)$$

with  $\langle \bar{\varphi} | \varphi \rangle = 0$ , and new energies

$$\Delta E_{\varphi, \bar{\varphi}} = \frac{J_1}{2} [1 \mp \sqrt{1 + 32M^2 J_c^2 / (3J_1^2)}], \quad (5)$$

with  $\tan \varphi = -\Delta E_{\varphi} \sqrt{6} / (4J_c M)$ .  $|\varphi\rangle$  is the ground state and  $|\bar{\varphi}\rangle$  can be identified as a longitudinal magnon excitation. The physical interpretation of this excitation is as follows. When  $J_c = 0$  we have isolated tetrahedra, and  $|\bar{\varphi}\rangle$  would correspond to the excited intratetrahedral triplet state  $|\psi_{t_{11}}^0\rangle$ . For  $J_c \neq 0$ ,  $|\bar{\varphi}\rangle$  evolves continuously from  $\psi_{t_{11}}$  as a function of the intertetrahedral coupling  $J_c$ , and becomes soft at the transition point to the ordered state. The molecular field also couples  $\psi_{t_{11}}$  with the quintuplet  $\psi_q$ , though we neglect this coupling here since we are interested in phases with low transition temperatures  $T_N$  for which the high-energy quintuplet does not contribute significantly.

The calculation of the staggered magnetization  $M = \text{Tr}[(S_1^z + S_2^z - S_3^z - S_4^z)e^{-\beta H}] / (4Z)$  [Eq. (3)] leads to the following self-consistency equation:

$$M = \frac{e^{-\beta E_{\varphi}} - e^{-\beta E_{\bar{\varphi}}}}{Z} \sqrt{\frac{2}{3}} \frac{\tan \varphi}{1 + \tan^2 \varphi}, \quad (6)$$

where  $\beta = 1/T$  and  $Z$  is the partition function for the coupled tetrahedra system, i.e.,  $Z = e^{-\beta E_{s_1}} + e^{-\beta E_{s_2}} + \dots$ . For  $J_c = J_c^{(qc)} = 3J_1/4$  the magnetization  $M$  goes to zero and the system shows a second-order phase transition at  $T_N$ .

## RESULTS

The transition temperature  $T_N$  can be obtained from Eq. (6) by imposing  $M = 0$ . Assuming that (i)  $s_2$  is the lowest excited state of a tetrahedron and (ii) at small temperatures only the leading order in a  $1/T$  expansion is contributing in Eq. (6),  $T_N$  can be analytically derived:

$$T_N \approx \Delta E_{s_2} \log^{-1} [J_c^{(qc)} / (J_c - J_c^{(qc)})]. \quad (7)$$

$T_N$  shows an inverse-log singularity close to the quantum critical point at  $J_c = J_c^{(qc)}$ . The critical  $J_c^{(qc)} = 3J_1/4$  is independent of  $J_2$ . In Fig. 2 we plot  $T_N$  as a function of  $J_c$ , both as obtained in the analytic solution Eq. (7) and by numerically solving the self-consistent equation (6). Note that for the region  $J_c \sim J_c^{(qc)}$ , Eq. (7) provides a good approximation for  $T_N$ .

The inverse-log dependence of the Néel temperature implies that  $T_N$  is substantial even near the quantum critical point, as illustrated in Fig. 2, in contrast to the magnitude of the zero-temperature magnetic moment,

$$M(T=0) = \frac{1}{\sqrt{6}} \sqrt{1 - (J_c^{(qc)} / J_c)^2}, \quad (8)$$

which has a standard mean-field form<sup>13</sup> (compare Fig. 2). For  $J_2 > J_1$  the tetrahedral ground state changes to  $\psi_{s_2}$  and the nonmagnetic singlet  $\psi_{s_2}$  therefore sets the scale for  $T_N$ .

## STATES IN AN EXTERNAL FIELD

An external longitudinal magnetic field does not induce additional couplings in between the different eigenstates, but it leads to shifts in the respective eigenenergies. A transversal magnetic field  $B_x$  induces, on the other hand, a coupling in between  $\psi_{i1}^0$  and  $\psi_{i1}^\pm$  [see Eq. (2)]. The mean-field ground state, which breaks the rotational invariance, can be written, in lowest order in  $B_x$ , as

$$|\varphi, B_x\rangle = \cos \alpha |\varphi\rangle + \frac{\sin \alpha}{\sqrt{2}} [|\psi_{i1}^+\rangle + |\psi_{i1}^-\rangle], \quad (9)$$

with  $\tan \alpha = B_x \sin \varphi / (J_1 - \Delta E_\varphi)$ . In lowest order in  $B_x$ , the ground-state energy  $\Delta E_{\varphi, B_x} = E_{\varphi, B_x} - E_\varphi$ ,

$$\Delta E_{\varphi, B_x} = -B_x^2 \sin^2 \varphi / (J_1 - \Delta E_\varphi), \quad (10)$$

decreases quadratically with  $B_x$ .

This result has an interesting consequence for the transition temperature. The energy of the excited singlet  $E_{s_2}$  is not affected by  $B_x$ : its relative energy to the ground state  $\Delta E_{s_2}$  increases consequently with  $B_x$  [compare Eq. (10)]. Equation (7) then tells us that the Néel temperature also increases with  $B_x$ .<sup>15</sup> An order-of-magnitude estimate of the effect for  $\text{Cu}_2\text{Te}_2\text{O}_5\text{Br}_2$  and  $B_x = 13$  T yields  $\Delta T_N \approx 0.8$  K  $= 0.56$  cm<sup>-1</sup>, which agrees well with the experimentally observed raise of  $\sim 1$  K already reported in Ref. 8.

For the longitudinal magnon, a calculation analogous to Eq. (10) leads to

$$\Delta E_{\bar{\varphi}, B_x} = -B_x^2 \cos^2 \varphi / (J_1 - \Delta E_{\bar{\varphi}}), \quad (11)$$

The resulting change  $\Delta E_{\bar{\varphi}, B_x} = E_{\bar{\varphi}, B_x} - E_{\bar{\varphi}}$  in the longitudinal-magnon energy is positive, as  $J_1 - \Delta E_{\bar{\varphi}} < 0$ , and substantially larger than the shift for the ground state  $\Delta E_{\varphi, B_x}$  (and correspondingly for  $E_{s_2}$ ) since  $\cos^2 \varphi \gg \sin^2 \varphi$ . As we shall discuss in the next sections, this trend is qualitatively in agreement with the Raman data presented below.

## SUBSTITUTION EXPERIMENTS

Specific heat and high-field magnetization have been measured on  $\text{Cu}_2\text{Te}_2\text{O}_5(\text{Br}_x\text{Cl}_{1-x})_2$  powder samples with  $x = 1, 0.75, 0.66$ , and  $0.0$ .<sup>7,8</sup> Substituting Br by Cl leads to a continuous decrease of the unit cell volume by 7% ( $x=0$ ) and an increase of the transition temperature from 11.4 to 18.2 K. Also, other physical properties change continuously with substitution.<sup>14</sup> In our coupled-cluster model we expect that the decrease of the unit cell volume causes an increase of the coupling constant  $J_c$ . We have calculated the specific heat

$$C_v = \beta^2 \langle (H - \langle H \rangle)^2 \rangle \quad (12)$$

in the mean-field approximation. In Fig. 3 the results are shown for various  $J_c$  values. In the inset of Fig. 3 the evolution of the experimentally determined specific heat as a function of substitution  $x$  is presented. Note that the mean-

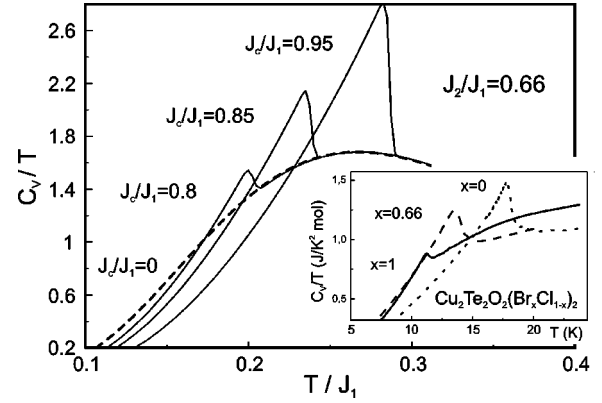


FIG. 3. Mean-field results for the specific heat of spin tetrahedra coupled by  $J_c$ . The inset shows the specific heat of  $\text{Cu}_2\text{Te}_2\text{O}_5(\text{Br}_x\text{Cl}_{1-x})_2$  with  $x = 1, 0.66$ , and  $0$ . The data with  $x = 0$  and  $1$  are compiled from Ref. 8.

field results for increasing  $J_c$  reproduce the continuous shift of the specific heat anomaly to higher temperatures with decreasing  $x$ .

A further support to the interpretation of these systems as that of coupled tetrahedra with a mean-field  $J_c$  intertetrahedra coupling and with a  $T_N$  ordering temperature is obtained from high-field magnetization measurements which are presented in Fig. 4. We observe a finite slope for all samples at small fields which increases with decreasing  $x$ , and no direct evidence for a plateau in the magnetization curve is found. A plateau at  $M = 1/2$  is predicted for a one-dimensional chain of spin tetrahedra with parameters placing the system in the gapped phase.<sup>10</sup> The absence of such a plateau in our experimental observations would support the fact that these systems cannot be described as chains of tetrahedra.<sup>11</sup> The finite slope in  $M(H)$  at small fields and even for  $x = 1$  is intrinsic, and points to the underlying weak Néel state. The corresponding anisotropy is observed in single crystal susceptibil-

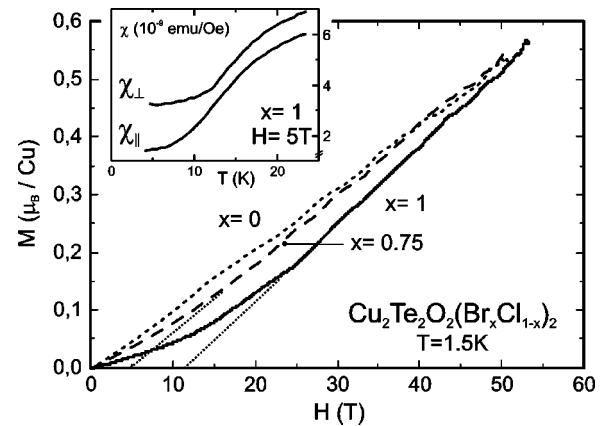


FIG. 4. High-field magnetization of  $\text{Cu}_2\text{Te}_2\text{O}_5(\text{Br}_x\text{Cl}_{1-x})_2$  powder samples for  $x = 1, 0.75$ , and  $0$ . The data with  $x = 0.66$  are omitted here for clarity. Dotted lines correspond to high field extrapolations. The kink in  $M(H, x=1)$  at  $H_{\text{SF}} = 13.2$  T is interpreted as a spin-flop transition. The inset shows the anisotropic magnetic susceptibility of  $\text{Cu}_2\text{Te}_2\text{O}_5\text{Br}_2$  single crystals.

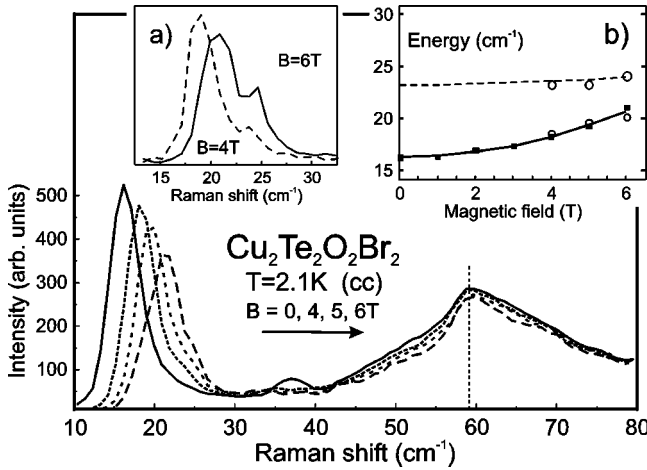


FIG. 5. Raman spectra of  $\text{Cu}_2\text{Te}_2\text{O}_5\text{Br}_2$  in a magnetic field. The insets show a) spectra with higher resolution and b) the shift of the  $\nu_{\text{sing}} = 23.2 \text{ cm}^{-1}$  mode (upper open symbols) and the  $\nu_{\text{long}} = 16.3 \text{ cm}^{-1}$  mode (lower full and open symbols) as a function of the magnetic field. The dashed line shows the field dependence of the transition temperature (Ref. 8), and the full line is a fit to the data proportional to the square of the magnetic field. The open (full) symbols show data with high resolution (normal resolution).

ity shown in the inset of Fig. 4. The transition is evident as a kink in  $\chi(T)$  with a magnetic field perpendicular to the  $c$ -axis.

### RAMAN SPECTROSCOPY

We have performed Raman scattering experiments on  $c$ -axis oriented single crystals with diameters  $\varnothing \approx 0.2 \text{ mm}$  and length  $l \approx 1 \text{ mm}$ . The used scattering geometry in (cc) light scattering polarizations corresponds to  $\mathbf{A}$  symmetry.<sup>8</sup> The magnetic field has been applied perpendicular to the light scattering polarization. In Fig. 5 we present Raman data for  $\text{Cu}_2\text{Te}_2\text{O}_5\text{Br}_2$  in magnetic fields up to 6 T. We observe a shift of the low-energy magnetic mode at  $\nu_{\text{long}} = 16.3 \text{ cm}^{-1} = 23.4 \text{ K}$  (for  $B=0$ ) to higher energies as a function of  $B$  and the appearance of an additional, magnetic field-induced mode at  $\nu_{\text{sing}} = 23.2 \text{ cm}^{-1} = 33.2 \text{ K}$  ( $B \neq 0$ ). In the inset Fig. 5(a) the low energy spectrum is displayed, with a smaller optical slit width and a higher spectral resolution. The intensity of the higher energy mode increases with field. It is not observable for  $B=0$ .

In Fig. 5(b) the energies of the respective modes are shown as a function of the magnetic field. While the higher energy mode does not show an appreciable magnetic field dependence (upper open symbols), the lower energy mode shows a nonlinear dependence on the magnetic field (lower full and open symbols). The full line in Fig. 5(b) is a fit to the data proportional to the square of the magnetic field. The dashed curve describing the higher energy mode is proportional to the weaker, positive field dependence of the transition temperature as determined by specific heat and magnetic susceptibility measurements.<sup>8</sup> In the following we shall argue that these two modes at  $\nu_{\text{long}} = 16.3 \text{ cm}^{-1}$  and  $\nu_{\text{sing}} = 23.2 \text{ cm}^{-1}$  can be identified as a longitudinal magnon

mode and as an excitation to the second singlet  $\psi_{s_2}$  in Eq. (1), respectively.

### EXCITED SINGLET

We interpret the additional higher energy mode at  $\nu_{\text{sing}} = 23.2 \text{ cm}^{-1}$  presented in Fig. 5 as a transition to the second singlet  $\psi_{s_2} = s_{12}s_{34}$ . Since this system is noncentrosymmetric, there is a nonzero Dzyaloshinski-Moriya (DM) (Ref. 16) interaction. Assuming a DM contribution to the Raman operator, i.e.,  $H_R^{(DM)} \sim \mathbf{D}_{ij} \cdot (\mathbf{S}_i \times \mathbf{S}_j)$  we find a nonzero Raman matrix element

$$\langle \psi_{s_2} | H_R^{(DM)} | \varphi, B^x \rangle \sim \sin \alpha \sim B^x M.$$

The  $23.2\text{-cm}^{-1}$ -mode would therefore be observable only in the ordered phase and in an external magnetic field, consistent with experiment. Having identified this mode with the transition to  $\psi_{s_2}$  we have then that

$$\Delta E_{s_2} = 2J_1 - 2J_2 = \nu_{\text{sing}} \sim 33 \text{ K}. \quad (13)$$

Considering Eq. (13) and the magnetic susceptibility<sup>7,8</sup> for  $T > T_N$  we find a good fit with  $J_1 \sim 47 \text{ K}$  and  $J_2 \sim 31 \text{ K}$  which yields  $J_2/J_1 \sim 0.66$ . The experimental transition temperature<sup>8</sup> of  $T_N^{(\text{Br})} = 11.4 \text{ K}$  for  $\text{Cu}_2\text{Te}_2\text{O}_5\text{Br}_2$  implies via self-consistency condition (6), that  $J_c \sim 0.85J_1$ .

Moreover, recalling Eqs. (7) and (10), for  $B_x = 6 \text{ T}$  the energy  $\Delta E_{s_2}$  of the excited singlet shifts by about  $0.12 \text{ cm}^{-1}$ . This increase is too small to be resolved by Raman, although the data presented in inset (b) of Fig. 5 seem to indicate a small increase.

### LONGITUDINAL MAGNON

We observe that the mean-field Hamiltonian [Eq. (3)] leads to a  $\mathbf{Q}=\mathbf{0}$  ordering for  $J_c > 0$ , and that the soft longitudinal magnon  $|\tilde{\varphi}\rangle$  should be directly observable in Raman scattering. For  $J_c < 0$  ordering with  $\mathbf{Q}=\pi$  would occur and additional backfolding to the zone center via residual lattice distortions would be necessary. The matrix element  $\langle \tilde{\varphi} | H_R | \varphi \rangle$  of the Raman operator  $H_R \sim \mathbf{S}_i \cdot \mathbf{S}_j$  ( $i, j = 1, \dots, 4$ ) is  $\sim \cos \varphi \sin \varphi$ . It vanishes in the decoupled-tetrahedra limit  $J_c = 0$ ,  $\varphi = 0$ , and the transition should be observable only in the ordered phase.

Summarizing, the Raman mode at  $\nu_{\text{long}} = 16.3 \text{ cm}^{-1} = 23.4 \text{ K}$  in Fig. 5 (i) has been shown<sup>8</sup> to become soft at the ordering temperature, and (ii) it is observable only in the condensed phase and its energy increases quadratically [compare Eq. (11)] with the field. We therefore interpret it as a longitudinal magnon.

The energy of this mode is strongly suppressed below its mean-field energy  $E_{\tilde{\varphi}} - E_{\varphi} = 54 \text{ K}$  by dispersion. We can estimate the magnitude of this suppression by comparison with the results of a bond-operator theory for a coupled dimer system<sup>17,18</sup> (alternatively one may use a generalized random phase approximation approach<sup>19</sup>). The effective dimer states are  $(\psi_{s_1}, \psi_{t_1}^{\alpha})$ . The gap of the longitudinal magnon has the form<sup>17</sup>

$$\Delta_{\text{long}} = \Delta_{\text{max}} \sqrt{1 - (J_c^{(qc)}/J_c)^2}. \quad (14)$$

For  $\text{Cu}_2\text{Te}_2\text{O}_5\text{Br}_2$  we have  $J_c = 0.85J_1$  [ $(J_c^{(qc)}/J_c)^2 = 0.78$ ] and  $\Delta_{\text{long}} \approx 0.47\Delta_{\text{max}}$ . The energy scale  $\Delta_{\text{max}}$  occurring in Eq. (14) is set by the longitudinal magnon gap in the classical Néel ordered state, i.e., in the limit of strong interdimer (tetrahedra) couplings, where it has the value  $\Delta_{\text{max}} \rightarrow J_c$ . With  $J_c \approx 0.85J_1$  and  $J_1 \approx 47$  K we then find for  $\text{Cu}_2\text{Te}_2\text{O}_5\text{Br}_2$  that  $\Delta_{\text{long}} \approx 19$  K, which is qualitatively in agreement with the experimental value  $\Delta_{\text{long}}^{(\text{expt})} = \nu_{\text{long}} = 23.4$  K; see the inset, Fig. 5(b). Due to the renormalization of  $\Delta_{\text{long}}$  by the fluctuations near the quantum-critical point [see Eq. (14)], we cannot easily quantitatively estimate its dependence on an external magnetic field, as presented in inset (b) of Fig. 5.

### COMPARISON WITH $\text{Cu}_2\text{Te}_2\text{O}_5\text{Cl}_2$

The magnitude of the intratetrahedral parameters have been estimated<sup>7</sup> from susceptibility measurements to be similar both for  $\text{Cu}_2\text{Te}_2\text{O}_5\text{Br}_2$  and the isostructural  $\text{Cu}_2\text{Te}_2\text{O}_5\text{Cl}_2$ . The substantially enhanced Néel temperature<sup>8</sup> of  $T_N^{(\text{Cl})} = 18.2$  K indicates a larger interdimer coupling for the Cl compound. This notion is consistent with the Raman results for doped compounds, which indicate a hardening of the excitations with the Cl content, as predicted by Eq. (14).<sup>14</sup> We did not attempt a quantitative analysis of the coupling parameters for  $\text{Cu}_2\text{Te}_2\text{O}_5\text{Cl}_2$  since we were not able to

observe the second singlet as in  $\text{Cu}_2\text{Te}_2\text{O}_5\text{Br}_2$ . Indeed, a generalized tight-binding analysis of band-structure calculations<sup>11</sup> indicates that the ratio of the intradimer couplings  $J_2/J_1$  in  $\text{Cu}_2\text{Te}_2\text{O}_5\text{Cl}_2$  is smaller than in  $\text{Cu}_2\text{Te}_2\text{O}_5\text{Br}_2$ . These findings also suggest that for  $\text{Cu}_2\text{Te}_2\text{O}_5\text{Cl}_2$  the excited singlet with energy  $E_{s2} = 2J_1 - 2J_2$  should probably be located in the energy range of the magnetic continuum and thus not be observable separately.

### CONCLUSIONS

We have presented a comprehensive set of theoretical and experimental data indicating that the isostructural spin-tetrahedral compounds  $\text{Cu}_2\text{Te}_2\text{O}_5(\text{Br}_x\text{Cl}_{1-x})_2$  constitute a series of systems with a systematic variation of the microscopic parameters with respect to a quantum critical transition. We have pointed out the importance of the low-lying singlet for the magnetic state, and reported the observation of a low-energy longitudinal magnon.

### ACKNOWLEDGMENT

We acknowledge the support of the German Science Foundation (DFG SP1073, SFB484), INTAS 01-278, and important discussions with Wolfram Brenig, Frederic Mila, Jens Jensen, and T. Saha-Dasgupta.

- <sup>1</sup>I. Affleck and G.F. Wellman, Phys. Rev. B **46**, 8934 (1992); H.J. Schulz, Phys. Rev. Lett. **77**, 2790 (1996); F.H.L. Essler, A.M. Tsvelik, and G. Delfino, Phys. Rev. B **56**, 11 001 (1997).
- <sup>2</sup>B. Lake, D.A. Tennant, and S.E. Nagler, Phys. Rev. Lett. **85**, 832 (2000).
- <sup>3</sup>A. Zheludev, M. Kenzelmann, S. Raymond, T. Masuda, K. Uchinokura, and S.-H. Lee, Phys. Rev. B **65**, 014402 (2002).
- <sup>4</sup>S. Raymond *et al.* Phys. Rev. Lett. **82**, 2382 (1999).
- <sup>5</sup>M. Enderle, Z. Tun, W.J.L. Buyers, and M. Steiner, Phys. Rev. B **59**, 4235 (1999).
- <sup>6</sup>P. Lemmens, C. Gros, and G. Güntherodt, Phys. Rep. **375**, 1 (2003).
- <sup>7</sup>M. Johnsson, K.W. Törnroos, F. Mila, and P. Millet, Chem. Mater. **12**, 2853 (2000).
- <sup>8</sup>P. Lemmens, K.-Y. Choi, E.E. Kaul, C. Geibel, K. Becker, W. Brenig, R. Valentí, C. Gros, M. Johnsson, P. Millet, and F. Mila, Phys. Rev. Lett. **87**, 227201 (2001).
- <sup>9</sup>W. Brenig and K.W. Becker, Phys. Rev. B **64**, 214413 (2001).
- <sup>10</sup>K. Totsuka and H.-J. Mikeska, Phys. Rev. B **66**, 054435 (2002).
- <sup>11</sup>R. Valentí, T. Saha-Dasgupta, C. Gros, and H. Rosner

cond-mat/0301119 (unpublished).

- <sup>12</sup>Other possible ordering patterns, like  $\langle S_1^z + S_2^z + S_3^z + S_4^z \rangle$ , lead to first-order phase transitions.
- <sup>13</sup>For  $J_c/J_1 \rightarrow \infty$  the coupling to the quintuplet  $\psi_q$  neglected in Eq. (8) would contribute and the zero- $T$  moment would take the mean-field value of 1/2.
- <sup>14</sup>P. Lemmens, K.-Y. Choi, A. Ionescu, J. Pommer, G. Güntherodt, R. Valentí, C. Gros, W. Brenig, M. Johnsson, P. Millet, and F. Mila, J. Phys. Chem. Solids **63/6-8**, 1115 (2002).
- <sup>15</sup>Note that there is a smaller decreasing contribution in  $B_x$  to the Néel temperature coming from the log-term in Eq. (7) due to an enhancement of the effective  $J_1$ .
- <sup>16</sup>I.J. Dzyaloshinskii, J. Phys. Chem. Solids **4**, 241 (1958); T. Moriya, Phys. Rev. **120**, 91 (1960).
- <sup>17</sup>T. Sommer, M. Vojta, and K.W. Becker, Eur. Phys. J. B **23**, 329 (2001).
- <sup>18</sup>B. Normand and T.M. Rice, Phys. Rev. B **56**, 8760 (1997).
- <sup>19</sup>J. Jensen and A.R. Mackintosh, *Rare Earth Magnetism: Structures and Excitations* (Oxford University Press, Oxford, 1991).